


Effect of Al₂O₃ Nanoparticles Additives on the Density, Saturated Vapor Pressure, Surface Tension and Viscosity of Isopropyl Alcohol

Vitaly Zhelezny¹  · Vladimir Geller¹ · Yury Semenyuk¹ ·
Artem Nikulin²  · Nikolai Lukianov¹ · Taras Lozovsky¹ ·
Mykola Shymchuk¹

Received: 4 August 2017 / Accepted: 15 January 2018 / Published online: 30 January 2018
© Springer Science+Business Media, LLC, part of Springer Nature 2018

Abstract This paper presents results of an experimental study of the density, saturated vapor pressure, surface tension and viscosity of Al₂O₃ nanoparticle colloidal solutions in isopropyl alcohol. Studies of the thermophysical properties of nanofluids were performed at various temperatures and concentrations of Al₂O₃ nanoparticles. The paper gives considerable attention to a turbidimetric analysis of the stability of nanofluid samples. Samples of nanofluids remained stable over the range of parameters of the experiments, ensuring the reliability of the thermophysical property data for the Al₂O₃ nanoparticle colloidal solutions in isopropyl alcohol. The studies show that the addition of Al₂O₃ nanoparticles leads to an increase of the density, saturated vapor pressure and viscosity, as well as a decrease for the surface tension of isopropyl alcohol. The information reported in this paper on the various thermophysical properties for the isopropyl alcohol/Al₂O₃ nanoparticle model system is useful for the development of thermodynamically consistent models for predicting properties of nanofluids and correct modeling of the heat exchange processes.

Keywords Al₂O₃ nanoparticles · Density · Isopropyl alcohol · Nanofluid · Stability · Surface tension · Vapor pressure · Viscosity

✉ Artem Nikulin
artem.nikulin@tecnico.ulisboa.pt

¹ Department of Thermophysics and Applied Ecology, Odessa National Academy of Food Technologies, 1/3 Dvoryanskaya, Str., Odessa 65082, Ukraine

² Center for Innovation, Technology and Policy Research, IN+, Instituto Superior Técnico, Av. Rovisco Pais 1, 1049-001 Lisboa, Portugal

1 Introduction

Recently, the influence of nanoparticles on the thermophysical properties of substances and heat exchange characteristics of working fluids and heat transfer media has attracted close attention of researchers. Despite of an abundance of published papers devoted to the investigation of nanofluids, the presented results require correct physical interpretation. Thus, it is still premature to use obtained experimental data for the modeling of thermophysical properties and heat exchange processes.

As was reported previously, in some cases an application of nanofluids may benefit to increase the efficiency of heat exchange processes [1,2]. It is obvious that a scientifically substantiated explanation for the results obtained is only possible if there is reliable information on the thermophysical properties for promising nanofluids. The lack of information for the identical samples of nanofluids for various thermophysical properties creates additional difficulties in the development of thermodynamically valid models for their prediction.

It should be noted that the influence of nanoparticles on the thermal conductivity and viscosity of the base liquid was studied in most of published papers devoted to the investigation of thermophysical properties of nanofluids [3,4]. As was shown in reviews [3,4], the presence of metal nanoparticles, metal oxides and carbon nanotubes in base liquids increases the thermal conductivity and viscosity. However, experimental data reported in the literature very often disagree both quantitatively and qualitatively even for identical thermodynamic systems [5–8].

There are several explanations for this situation. First, there are few publications where authors pay sufficient attention to the stability of nanofluids under experimental conditions (over a wide range of temperatures and concentrations of nanoparticles). Given that nanofluids are colloidal solutions, their stability is dependent on the temperature. Second, properties of nanofluids are affected not only by the concentration of the colloidal solution components but also by nanoparticle size and shape, presence of surfactants and methods used for preparation of the nanofluids. Third, the techniques/experimental methods employed improperly may also explain the discrepancies of obtained experimental data reported by different authors, as was discussed in [9,10].

Thus, the various effects of nanoparticles presence on the properties of nanofluids are determined by combined influence of factors mentioned above. Moreover, as several authors have noted (see, for example, Choi et al. [11]), that the stability of colloidal solutions under experimental conditions is the decisive factor determining the accuracy of the experimental data on thermophysical properties of nanofluids. Stability of nanofluids is a key problem in the physical interpretation of the results obtained in the experimental study of the heat exchange processes or estimating parameters of the power plant efficiency. It should be mentioned that the information for the nanofluid properties such as the surface tension [7,12,13] or saturated vapor pressure [13,14], that are critical for the practical application of nanofluids is rather scant in existing literature.

Keeping previous in mind, it can be concluded that despite of the variety of papers devoted to study of the viscosity and thermal conductivity of nanofluids, the evaluation of the complex effect related with nanoparticles presence in solution on the thermo-

Table 1 Sample table

Chemical name	Source	Initial mole fraction purity	Purification method	Analysis method
Isopropanol/Al ₂ O ₃ (dispersion)	Aldrich	–	–	–
Aluminum oxide (nanoparticles)	Aldrich	0.999	–	TMA ^a
Isopropanol	Aldrich	0.997	–	GC ^b

^a Trace metal analysis^b Gas chromatography

physical properties are not yet resolved. The existing correlations for prediction of the thermophysical properties of the nanofluids do not provide sufficiently accurate information for the thermophysical properties of nanofluids, that necessary for their practical applications. Therefore, the purpose of the present work is an experimental study of the density, saturated vapor pressure, surface tension and viscosity for the model nanofluid with Al₂O₃ (aluminum oxide) nanoparticles in isopropyl alcohol.

2 Experimental, Results and Discussion

2.1 Preparation and Stability of the Nanofluid

2.1.1 Preparation of the Nanofluid

Sigma-Aldrich isopropanol/Al₂O₃ nanofluid (Product Number 702129) with a nanoparticle content of 20 ± 1 mass% was used in this study. This nanofluid was chosen because isopropanol forms stable over time colloidal solutions with Al₂O₃ nanoparticles over a wide range of concentrations and temperatures. According to the manufacturer, the size of the Al₂O₃ nanoparticles (CAS 1344-28-1) was not > 50 nm (DLS (dynamic light scattering)) with a purity of 99.9 % (Trace Metals Analysis). Samples were prepared by diluting the 702129 Aldrich nanofluid with isopropyl alcohol (CAS 67-63-0; 99.7 % pure (gas chromatography)). Diluted nanofluid was homogenized by simple, short-term mechanical shaking. All chemical samples are described in Table 1.

The exact quantity of nanofluid components was determined by a gravimetric method. An A&D GR-300 analytical scale with an uncertainty of ±0.4 mg was used.

The mass fraction of nanoparticles in the samples was determined by the following equation:

$$w_{\text{Al}_2\text{O}_3} = \frac{m_{\text{nf}} \cdot w_{\text{nf}}}{m_{\text{nf}} + m_{\text{ia}} - m''_{\text{ia}}} = \frac{m_{\text{Al}_2\text{O}_3}}{m_{\text{Al}_2\text{O}_3} + m_{\text{ia}} - m''_{\text{ia}}}, \quad (1)$$

where m_{nf} is the mass of the nanofluid, kg; $w_{\text{nf}} = 0.2$ mass fraction of nanoparticles in nanofluid, kg · kg⁻¹; $m_{\text{Al}_2\text{O}_3}$ is the mass of nanoparticles, kg; m_{ia} is the mass of isopropyl alcohol, kg; m''_{ia} is the mass of the vapor phase of isopropyl alcohol, kg.

Table 2 Experimental parameter ranges

Property	Stability	ρ	P	σ	ν
Temperature/K	298–343	263–343	298–363	293–343	293–343
Mass fraction of nanoparticles/%	0.036				
	0.050	0.92			0.12
	0.091	1.81	0.051		5.00
	0.433	4.01	0.108	0.566	11.07
	1.050	6.65	0.506	0.872	11.12
	4.212				

Standard uncertainty $u(w_{\text{Al}_2\text{O}_3}) = 2 \cdot 10^{-5} \text{ kg} \cdot \text{kg}^{-1}$

In the density, surface tension and saturated vapor pressure experiments the mass fraction of nanoparticles in the nanofluid in the measuring cell was determined by considering the mass of isopropyl alcohol in the vapor phase (1) using data on the total volume of the measuring cell and data on the isopropanol vapor density taken from Stephan et al. [15]

$$m''_{\text{ia}} = \rho''_{\text{ia}} (V_0 - V'_{\text{nf}}), \quad (2)$$

where ρ''_{ia} is the density of the vapor phase of isopropyl alcohol, $\text{kg} \cdot \text{m}^{-3}$; V_0 is the total volume of the measuring cell, m^3 ; V'_{nf} is the volume of the nanofluid liquid phase, m^3 .

The relationship between the mass of nanofluid and the mass of isopropyl alcohol in formula (1) is expressed as follows:

$$\frac{m_{\text{ia}}}{m_{\text{nf}}} = \frac{w_{\text{nf}}}{w_{\text{Al}_2\text{O}_3}} - 1, \quad (3)$$

where w_{nf} is mass fraction of nanoparticles to be obtained when preparing the test sample, $\text{kg} \cdot \text{kg}^{-1}$.

The simplicity of the procedure for nanofluid preparation, as well as the fact that this nanofluid is industrially manufactured, makes it an attractive object for further studies. This method allows to eliminate complicating factors for the result analyses such as the nanoparticle size, method of preparation of nanofluids, effect of surfactants on the property or the process and purity of the materials used to prepare the nanofluids. This makes it possible to compare the data obtained by different authors under different experimental conditions.

The experimental parameters in which measurements were taken for each property are given in Table 2.

Experimental parameters were determined based on the issues encountered in previous studies on the heat exchange processes occurring in the boiling nanofluids [16] and formation of the database for development of nanofluid property prediction methods [17].

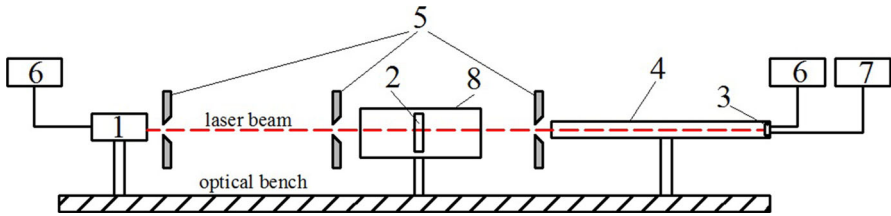


Fig. 1 Scheme of the experimental apparatus for determining nanofluid stability: 1 laser; 2 optic cell; 3 photodiode; 4 tube; 5 optical gaps; 6 stabilized power sources; 7 multimeter

2.1.2 Experimental Setup for the Study of Nanofluid Stability

The stability of nanofluids determines the potential for practical application of nanotechnologies in power engineering. The processes of sedimentation stability can also influence the severity of the effects of nanoparticles on the properties of base fluids or for the heat exchange and parameters of equipment efficiency [11].

The experimental setup for the study of nanofluid stability is shown in Fig. 1. A laser (1; 650 nm wavelength) was used as a light source. The laser beam passes through the optic cell (2) with two plane-parallel glasses (optical path length l). Following passage through the nanofluid, the laser ray reaches a photodiode (3; OPT101). To prevent scattered light from entering to the photodiode, the latter was placed in a tube (4) that was coated on the inside using a material with a high light absorption coefficient. To obtain a parallel light beam with a diameter of 2 mm, optical gaps (5) were used. The laser and the photodiode were powered by stabilized power sources (6). The signals from the photodiode were registered (in V) by a multimeter RIGOL DM3064 (7). To maintain the required temperature, the optic cell was placed in a thermostat (8), which was a massive cylindrical copper block through which coolant was pumped from an auxiliary thermostat (not shown in the diagram).

The procedure for determining the stability of nanofluids included several stages. First, the maximum signal U_{\max} (V) received from the photodiode was measured in the absence of the sample. After filling cell (2) with the sample, signal U_{nano} (V) was measured. Considering possible changes in the laser characteristics, the magnitude of nanofluid stability was expressed as the ratio $U_{\text{ratio}} = U_{\text{nano}}/U_{\max}$.

To exclude the effect of the light source parameters on the measured values of U_{ratio} when determining its concentration dependence, the value U_{ratio} was calculated as $U_{\text{ratio}} = U_{\text{nano}}/U_{\text{base}}$. The value of U_{base} was measured when the optic cell contained only pure isopropanol. The uncertainty of the U_{ratio} value did not exceed ± 0.008 (0.95 confidence interval).

2.1.3 Results for the Nanofluid Stability

To study the sedimentation stability of the isopropanol/ Al_2O_3 nanofluid, a sample with a 0.05 % mass fraction of nanoparticles in a cell with optical path length $l = 100$ mm was used. As is shown in Fig. 2, sedimentation was not observed in the nanofluid at least for 100 h.

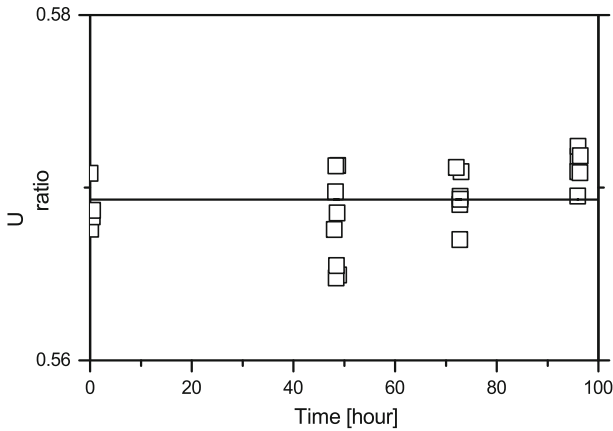


Fig. 2 U_{ratio} value for the isopropanol/ Al_2O_3 nanofluid as a function of time with an optical path length of the cell $l = 100$ mm (\square) $w_{\text{Al}_2\text{O}_3} = 0.05$ mass%

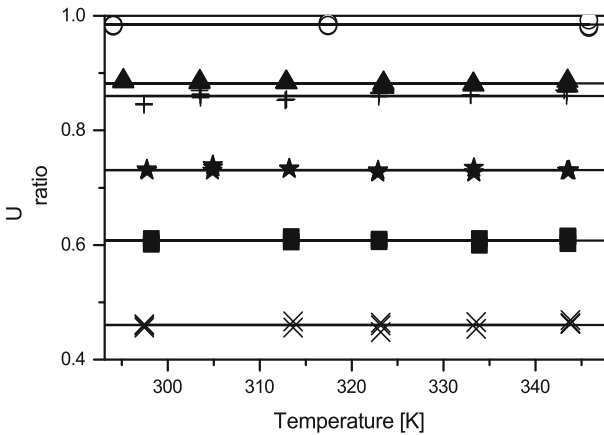


Fig. 3 U_{ratio} value for isopropanol/ Al_2O_3 nanofluid as a function of temperature T with an optical path length of the cell $l = 4.5$ mm (\circ) $w_{\text{Al}_2\text{O}_3} = 0$ mass%; (\blacktriangle) $w_{\text{Al}_2\text{O}_3} = 0.036$ mass%; ($+$) $w_{\text{Al}_2\text{O}_3} = 0.091$ mass%; (\star) $w_{\text{Al}_2\text{O}_3} = 0.433$ mass%; (\blacksquare) $w_{\text{Al}_2\text{O}_3} = 1.050$ mass%; (\times) $w_{\text{Al}_2\text{O}_3} = 4.212$ mass%

Additional experiments were carried out to study the effect of the temperature (from 290 K to 343 K) on the nanofluid stability (Fig. 3). The nanofluid was placed in a cell with optical path length $l = 4.5$ mm and was held at each temperature for at least 1 h. As shown in Fig. 3, the studied isopropanol/ Al_2O_3 nanofluid samples are stable at concentrations up to 4.2 mass%.

As shown in Figs. 2 and 3, the isopropanol/ Al_2O_3 nanofluid remained stable over the entire study period. This is confirmed by the pictures (Fig. 4) of the samples that were held for approximately 200 h at a temperature of 348 K.

Analysis of the experimental results shows that nanofluids obtained by diluting 702129 Aldrich nanofluid sample with isopropyl alcohol were stable over studied range of the time, temperatures and nanoparticle concentrations. The use of nanofluid

Fig. 4 Samples of the isopropanol/ Al_2O_3 nanofluid ($w_{\text{Al}_2\text{O}_3} = 4.2 \text{ mass\%}$): (a) immediately after preparation; (b) after 200 h at 348 K



samples prepared by this method significantly increases the reliability of the obtained information for the thermophysical properties of nanofluids.

2.2 Density Study

The density measurements of nanofluid samples were taken using a variable volume pycnometer. The pycnometer was placed in a thermostat equipped with an automatic temperature control system where the temperature fluctuations in the thermostat did not exceed 0.02 K. To measure the height of the sample's meniscus in the pycnometer, a KM-8 cathetometer with a height measuring an uncertainty of $\pm 0.02 \text{ mm}$ was used. The experiment was carried out in temperature range 263 K to 343 K with mass fractions of nanoparticles between 0 % and 6.65 %. Prior to the density study, the pycnometer was calibrated with pure isopropanol. The density data for the pure isopropanol were taken from Stephan et al. [15].

The experimental data for the nanofluid density are given in Table 3 and Fig. 5.

Experimental data for the density of nanofluid were fitted by following equation.

$$\rho(T) = \exp(a + b \cdot T^2), \quad (4)$$

where a and b are coefficients dependent on the mass fraction of nanoparticles (see Table 4).

Figure 6 shows the absolute density deviations from pure isopropanol for isopropanol/ Al_2O_3 nanofluids as a function of the concentration of nanoparticles at equal temperatures.

As shown in Fig. 6, the nanofluid density increases with increase of the nanoparticle concentration. An increase in temperature leads to a slight weakening of this effect. For example, at 0.9 mass% of nanoparticles and temperature of 263 K, the density

Table 3 Experimental density values, ρ , as a function of temperature and mass fraction of nanoparticles $w_{\text{Al}_2\text{O}_3}$ for isopropanol/ Al_2O_3 nanofluid

	T/K	$w_{\text{Al}_2\text{O}_3}/\text{mass}\%$	$\rho/\text{kg} \cdot \text{m}^{-3}$
	263.1	–	810.9
	283.1	–	795.3
	295.3	–	784.3
	303.6	–	777.5
	323.4	–	760.1
	343.3	–	741.0
	263.1	0.917	816.9
	283.3	0.917	800.7
	303.5	0.917	783.5
	323.2	0.917	765.7
	343.2	0.917	746.7
	262.9	1.811	827.5
	283.2	1.811	811.4
	303.2	1.811	793.1
	323.1	1.811	775.1
	342.9	1.811	755.8
	263.1	4.008	843.8
	283.0	4.008	827.8
	303.2	4.008	809.3
	323.1	4.008	791.2
	343.2	4.008	771.6
	263.1	6.646	859.9
	283.3	6.646	843.6
Standard uncertainty	303.3	6.646	826.0
$u(T) = 0.1 \text{ K}$. Expanded	323.1	6.646	807.9
uncertainty	343.2	6.646	788.1
$U(\rho) = 1.0 \text{ kg} \cdot \text{m}^{-3}$ (0.95 level			
of confidence)			

increases for $10.6 \text{ kg} \cdot \text{m}^{-3}$ (1.31 %), and at temperature of 353 K, the increase of the density was $8.4 \text{ kg} \cdot \text{m}^{-3}$ (1.14 %). The maximum absolute effect of $49.1 \text{ kg} \cdot \text{m}^{-3}$ (6.6 %) was obtained with a mass fraction of nanoparticles equal to 6.6 mass% at the temperature of 263 K. It should be mentioned that the data obtained are in qualitative agreement with data reported by Vajjha et al. [18].

2.3 Saturated Vapor Pressure Study

Studies of the saturated vapor pressure of isopropanol and isopropanol/ Al_2O_3 nanofluid were conducted in temperature range between 298 K and 363 K. The experimental apparatus was previously described in Zhelezny et al. [13]. In order to measure the saturated vapor pressure of nanofluids, a WIKA S-10 pressure transducer with a 0 to 1×10^5 Pa measured pressure range was used.

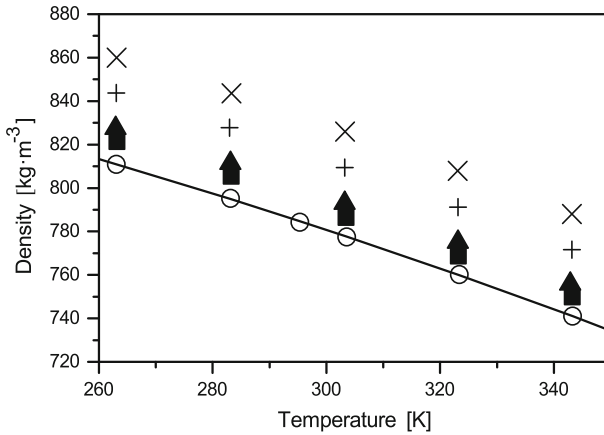


Fig. 5 Density ρ as a function of temperature T and mass fraction of nanoparticles $w_{Al_2O_3}$ for isopropanol/ Al_2O_3 nanofluid (—) isopropanol [15]; (○) $w_{Al_2O_3} = 0$ mass%; (■) $w_{Al_2O_3} = 0.917$ mass%; (▲) $w_{Al_2O_3} = 1.811$ mass%; (+) $w_{Al_2O_3} = 4.008$ mass%; (×) $w_{Al_2O_3} = 6.646$ mass%

Table 4 Coefficients a and b in Eq. 4

$w/\text{mass}\%$	a	b	r^2	Fit. SE
0.000	6.8266	$-1.8518E-06$	0.99983	0.36
0.917	6.8420	$-1.8865E-06$	0.99970	0.57
1.811	6.8484	$-1.8742E-06$	0.99984	0.42
4.008	6.8660	$-1.8455E-06$	0.99989	0.35
6.646	6.8814	$-1.7943E-06$	0.99987	0.37

The experimental data on the pressure of isopropanol and isopropanol/ Al_2O_3 nanofluids are listed in Table 5.

Experimental data on the saturated vapor pressure were fitted by equation:

$$P(T) = \exp(a + b/T), \tag{5}$$

where a and b are coefficients that depend on the mass fraction of nanoparticles (see Table 6).

It should be stated here that the experimental uncertainty is higher than obtained effects of influence of nanoparticle additives on the saturated vapor pressure for investigated colloidal solutions. However, it should not be considered during comparison of the results obtained using the same experimental setup within frame of the same experiments. In addition, each data point presented in Table 5 is an average value for at least 20 data readings. All data were used in fitting process and the calculated confidence interval at 0.95 confidence level was no $> \pm 70$ Pa at the highest temperature. After careful analysis of the calculated results, we can conclude that the additives of nanoparticles lead to a slight increase of the saturated vapor pressure for the isopropanol/ Al_2O_3 nanofluid (see Fig. 7).

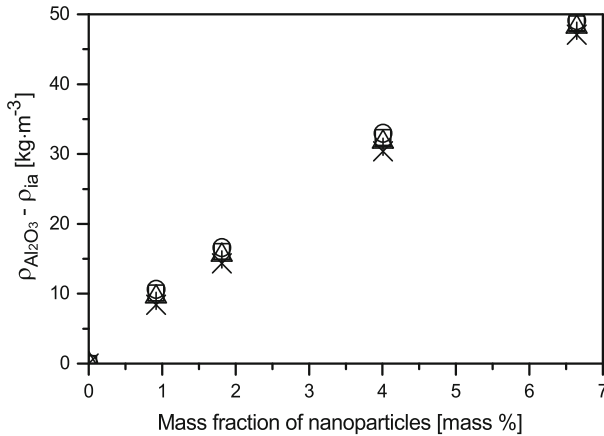


Fig. 6 Absolute deviations $\Delta\rho = \rho_{Al_2O_3} - \rho_{ia}$ of density $\rho_{Al_2O_3}$ of isopropanol/ Al_2O_3 nanofluids from the density ρ_{ia} of pure isopropanol at various temperatures (o) $T = 263$ K; (□) $T = 283$ K; (Δ) $T = 303$ K; (+) $T = 323$ K; (×) $T = 353$ K

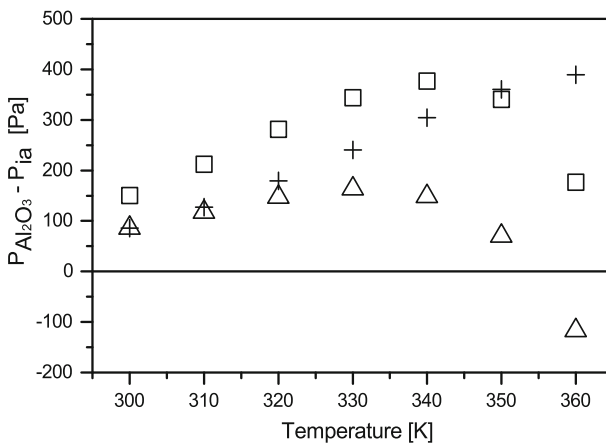


Fig. 7 Absolute deviations $\Delta P = P_{Al_2O_3} - P_{ia}$ of saturated vapor pressure $P_{Al_2O_3}$ for the isopropanol/ Al_2O_3 nanofluid from the saturated vapor pressure P_{ia} of pure isopropanol at various mass fractions: (□) $w_{Al_2O_3} = 0.051$ mass%; (Δ) $w_{Al_2O_3} = 0.108$ mass%; (+) $w_{Al_2O_3} = 0.506$ mass%

Absolute deviations of the saturated vapor pressure values of nanofluid calculated by Eq. 5 from the saturated vapor pressure values of pure isopropanol are shown in Fig. 7.

As determined from the previous results, the addition of Al_2O_3 nanoparticles to isopropyl alcohol causes an increase in the saturated vapor pressure. The relative effect of the nanoparticles on the pressure was greatest at low temperatures, up to 3.5% at $w_{Al_2O_3} = 0.051$ mass%. As the temperature increases, the relative effect of Al_2O_3 nanoparticles presence decreases. At temperatures above 350 K, the effect of nanoparticles presence on the vapor pressure does not exceed 1%.

Table 5 Experimental values of the saturated vapor pressure P as a function of the temperature T and the mass fraction of nanoparticles $w_{Al_2O_3}$ for the isopropanol/ Al_2O_3 nanofluid

T/K	$w/mass\%$	P/kPa
297.8	0	6.38
303.6	0	8.93
321.1	0	21.91
333.4	0	39.46
343.3	0	61.57
352.8	0	92.28
362.5	0	134.96
303.3	0.051	9.62
323.4	0.051	25.33
332.2	0.051	37.69
343.2	0.051	61.76
351.9	0.051	89.09
361.5	0.051	130.09
299.2	0.108	7.26
306.5	0.108	10.84
323.8	0.108	25.43
325.7	0.108	27.73
334.8	0.108	42.39
343.4	0.108	62.21
354.7	0.108	99.86
363.0	0.108	137.33
299.5	0.506	7.20
303.5	0.506	9.09
324.1	0.506	26.12
333.9	0.506	40.61
341.5	0.506	57.39
353.3	0.506	94.31
362.3	0.506	134.59

Standard uncertainty $u(T) = 0.1$ K. Expanded uncertainty $U(P) = 1.0$ kPa (0.95 level of confidence)

Table 6 Coefficients a and b for Eq. 5

$w/mass\%$	a	b	r^2	Fit. SE
0	25.831	-5093.5	0.99998	185
0.051	25.738	-5032.8	0.99995	258
0.108	25.767	-5049.2	0.99997	225
0.506	25.792	-5068.4	0.99998	197

The results obtained in presented study agree qualitatively with results reported in [13, 14]. Xu et al. [14] examined the saturated vapor pressure of HFC134a/mineral oil solutions at presence of Fe_3O_4 nanoparticles. The saturated vapor pressure was measured between 263 K and 328 K. The reported results by Xu et al. [14] showed that the vapor pressure of the refrigerant/oil solution (ROS) with nanoparticles was

higher than vapor pressure for the pure ROS over entire temperature range, with an average deviation of 7.61 % and maximum of 17.65 %. Unfortunately, this paper does not contain detailed information on the methods of nanofluid sample preparation and its stability. It also lacks data on the concentration of nanoparticles and their size, so reported information should be used with some caution.

More detailed studies were performed by Zhelezny et al. [13]. The authors studied the effect of Al_2O_3 and TiO_2 nanoparticle additives (0.5 mass%) on the saturated vapor pressure of isobutane–mineral oil solutions between 275 K and 353 K at different oil concentrations. Preliminary studies of these nanofluids by a spectral turbidimetric method showed that under mixing, the average nanoparticle radius (approximately 130 nm) remains unchanged for at least 200 h. The presence of Al_2O_3 and TiO_2 nanoparticles (0.5 mass%) in ROS leads to an increase of the saturated vapor pressure. The effect of nanoparticles on the saturated vapor pressure of the ROS was dependent from temperature and concentration.

2.4 Surface Tension Study

Measurements on the surface tension for the nanofluids were taken in the temperature range of 290–345 K using the experimental apparatus described in Zhelezny et al. [13]. The experimental apparatus implements differential capillary rise method, which was reported in Zhelezny et al. [19].

The capillary constant and surface tension experimental data are listed in Table 7. When calculating isopropanol and nanoisopropanol surface tension values, the density for the pure isopropanol was taken from Stephan et al. [15].

The experimental data on the capillary constant and surface tension were fitted by equation:

$$y(T) = c + d \cdot T, \quad (6)$$

where y is the capillary constant a^2 , mm^2 or surface tension σ , $\text{mN} \cdot \text{m}^{-1}$; c and d are the coefficients dependent on the mass fraction of nanoparticles (see Table 8).

The absolute deviations of the isopropanol/ Al_2O_3 nanofluid capillary constant and surface tension values from those values for pure isopropanol calculated by formula (6) are shown in Fig. 8. It can be concluded that the presence of Al_2O_3 nanoparticles in isopropanol leads to decrease of the surface tension. Moreover, the effect is greater when concentration of nanoparticles in isopropanol was $w_{\text{Al}_2\text{O}_3} = 0.566$ mass%. The effect for the capillary constant was found between 0.09 mm^2 and 0.22 mm^2 , and for the surface tension from $0.36 \text{ mN} \cdot \text{m}^{-2}$ to $0.8 \text{ mN} \cdot \text{m}^{-2}$. At the concentration of Al_2O_3 nanoparticles in isopropanol $w_{\text{Al}_2\text{O}_3} = 0.872$ mass%, the effect was found from 0.03 mm^2 to 0.04 mm^2 for the capillary constant, for the surface tension from $0.12 \text{ mN} \cdot \text{m}^{-2}$ to $0.15 \text{ mN} \cdot \text{m}^{-2}$ correspondingly. The effect of nanoparticle concentration on surface tension is clearly complex. The temperature dependences of the surface tension for the nanofluid and the base fluid are similar.

Figure 9 shows the concentration dependence of the surface tension.

Table 7 Experimental values of the capillary constant a^2 and surface tension σ as a function of temperature T and mass fraction of nanoparticles $w_{\text{Al}_2\text{O}_3}$ for isopropanol/ Al_2O_3 nanofluid

Standard uncertainty
 $u(T) = 0.1$ K. Expanded
 uncertainty
 $U(a^2) = 0.032$ mm²,
 $U(\sigma) = 0.21$ mN · m⁻¹ (0.95
 level of confidence)

T/K	$w_{\text{Al}_2\text{O}_3}/\text{mass}\%$	a^2/mm^2	$\sigma/\text{mN} \cdot \text{m}^{-1}$
293.2	0	5.531	21.4
303.3	0	5.390	20.6
313.2	0	5.253	19.8
323.3	0	5.111	19.0
333.2	0	4.967	18.2
343.3	0	4.815	17.4
293.2	0.567	5.379	20.8
303.3	0.567	5.253	20.1
313.2	0.567	5.191	19.6
323.3	0.567	5.028	18.7
333.2	0.568	4.720	17.3
343.3	0.568	4.552	16.4
293.2	0.871	5.519	21.3
303.3	0.871	5.334	20.3
313.2	0.872	5.221	19.7
323.3	0.872	5.080	18.9
333.2	0.872	4.920	18.1

Table 8 Coefficients c and d for Eq. 6

$w/\text{mass}\%$	c	d	r^2	Fit. SE
a^2				
0	9.741	-0.01435	0.99968	0.005
0.567	10.38	-0.01683	0.95179	0.079
0.871	9.753	-0.01450	0.99409	0.020
σ				
0	44.74	-0.07959	0.99989	0.017
0.567	46.92	-0.08826	0.97599	0.290
0.871	44.77	-0.08011	0.99699	0.080

Obtained experimental results agreed qualitatively with results reported by Vafaei et al. [20]. The authors found that adding Bi_2Te_3 nanoparticles (2.5 nm and 10.4 nm) to water initially leads to decrease of the surface tension, but further increases the concentration of nanoparticles lead to opposite effect—increasing the surface tension values.

The study of Tanvir and Qiao [12] was focused on the surface tension of n -decane/ Al_2O_3 , n -decane/ Al , and n -decane/ B nanofluids with sorbitan oleate surfactant. Tanvir and Qiao [12] observed a similar effect. The surface tension decreases and then increases with increasing nanoparticle concentration. The authors noted that the increase in surfactant concentration in the nanofluid results in the decrease of the surface tension. For water/ Al_2O_3 , ethanol/ Al_2O_3 , ethanol/ Al and ethanol/ B nanofluids, higher concentrations of nanoparticles resulted in higher surface tension values.

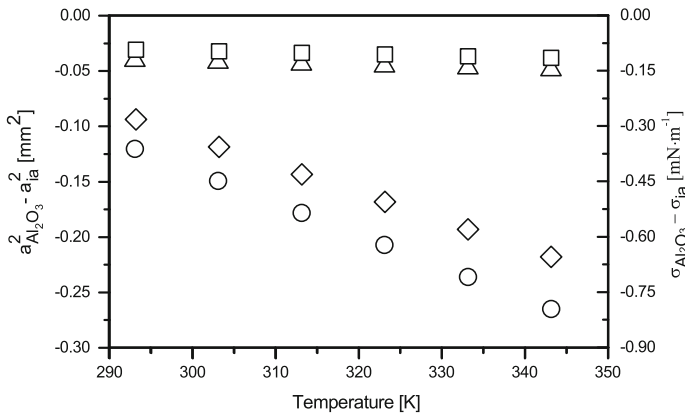


Fig. 8 Absolute deviations $\Delta a^2 = a_{Al_2O_3}^2 - a_{ia}^2$ of the isopropanol/ Al_2O_3 nanofluid capillary constant $a_{Al_2O_3}^2$ from capillary constant values a_{ia}^2 for pure isopropanol and absolute deviations $\Delta \sigma = \sigma_{Al_2O_3} - \sigma_{ia}$ of the isopropanol/ Al_2O_3 nanofluid surface tension $\sigma_{Al_2O_3}$ from pure isopropanol surface tension values σ_{ia} at various mass fractions: (\square) a^2 at $w_{Al_2O_3} = 0.871$ mass%; (\diamond) a^2 at $w_{Al_2O_3} = 0.567$ mass%; (Δ) σ for $w_{Al_2O_3} = 0.871$ mass%; (\circ) σ for $w_{Al_2O_3} = 0.567$ mass%

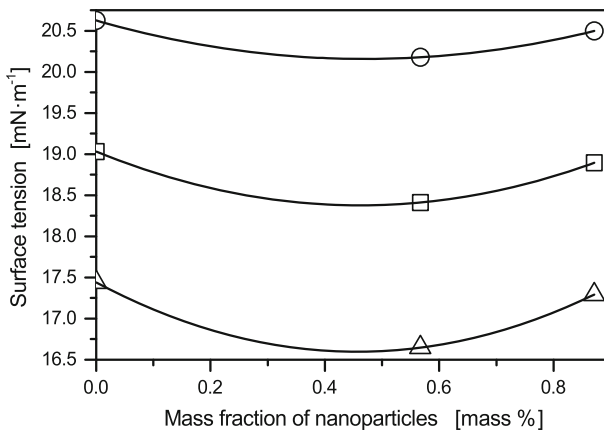


Fig. 9 Surface tension σ as a function of the mass fraction of nanoparticles $w_{Al_2O_3}$ and temperature T for the isopropanol/ Al_2O_3 nanofluid: (\circ) $T = 303$ K; (\square) $T = 323$ K; (Δ) $T = 343$ K

The results of decreasing the surface tension in water/ TiO_2 and graphene/water nanofluids are demonstrated by Murshed et al. [7] and Ahammed et al. [21]. In contrast, increase of the surface tension was observed in paper of Bhuiyan et al. [8] with the addition of Al_2O_3 , TiO_2 and SiO_2 nanoparticles to water.

Unfortunately, absence of data on the stability for the investigated nanofluids, as well as use of surfactants in some experiments, makes it difficult to analyze the reported information in previously mentioned papers.

The detailed study of the influence of Al_2O_3 and TiO_2 nanoparticles on the surface tension of isobutane solutions with mineral compressor oil is presented in Zhelezny et al. [13]. In this study was found, that addition of nanoparticles contributes to the

decrease of the surface tension for the base fluid. However, the authors emphasized that in analysis and modeling of the surface tension and saturated vapor pressure, both properties should be attributed to the concentration of the surface layer of solution and not to the composition of the solution in a liquid phase.

2.5 Viscosity Study

Viscosity measurements for the nanofluid samples were taken in temperature range between 293 K and 343 K using an experimental setup principally composed a glass capillary viscometer with a suspended level. This experimental method was widely applied for investigation of the nanofluid viscosity (for example, see references [6, 22–24]). However, well-known fact that some nanofluids (especially with very high concentration of nanoparticles) may demonstrate non-Newtonian behavior (Tertsinidou et al. [9]), and therefore, the capillary viscometers cannot be applied for the measurements. But, the results obtained by Sommers and Yerkes [25] have shown that for nanofluids with shear-thinning non-Newtonian behavior with the nanoparticles load up to 3 % by mass, the application of capillary viscometer and rotational rheometer gives the same results. In addition, Chen et al. [26] measured the viscosity of ethylene glycol/TiO₂ nanofluids and Newtonian behavior was confirmed up to 8 mass% fraction of nanoparticles.

During experiments, the temperature fluctuations in the thermostat did not exceed 0.02 K. All measurements were carried out repeatedly to reduce the influence of the random variations. Before carrying out experiments for the viscosity determination, the viscometers were calibrated against pure isopropanol and validated against previous data reported by Stephan et al. [15].

The viscosity measurements of isopropyl alcohol/Al₂O₃ nanofluids are presented in Table 9 and Figs. 10 and 11.

Analysis of the measurement results given in Figs. 10 and 11 shows that the presence of nanoparticles substantially increases the viscosity of the studied nanofluids, by approximately 50 % per 5 mass% of nanoparticles. In contrast, the temperature dependence of nanofluids is similar to the temperature dependence of the base fluid and the effect of nanoparticles presence on the viscosity depends on temperature. This can be explained by a change in the nanofluid structure when the temperature and mobility of the particles increase. This change corresponds to a decrease in the hydrodynamic radius of the particle which in turn leads to a decrease in the influence of nanoparticles on the viscosity of the base fluid. The experimental data were fitted as a dependent on the ratio $\nu_{\text{Al}_2\text{O}_3}/\nu_{\text{ia}}$, the temperature and the mass fraction $w_{\text{Al}_2\text{O}_3}$ of nanoparticles.

$$\frac{\nu_{\text{Al}_2\text{O}_3}}{\nu_{\text{ia}}}(T, w_{\text{Al}_2\text{O}_3}) = 1 + (41.52 - 90.16 \cdot 10^{-3}T)w_{\text{Al}_2\text{O}_3}, \quad (7)$$

where $\nu_{\text{Al}_2\text{O}_3}$ and ν_{ia} are the kinematic viscosity of the isopropanol/Al₂O₃ nanofluid and isopropanol, respectively, mm²·s⁻¹; T is the temperature, K; $w_{\text{Al}_2\text{O}_3}$ is the mass fraction of nanoparticles, kg · kg⁻¹.

Table 9 Experimental values of the viscosity ν as a function of temperature T and mass fraction of nanoparticles $w_{\text{Al}_2\text{O}_3}$ for isopropanol/ Al_2O_3 nanofluid

T/K	$w/\text{mass}\%$	$\nu/\text{mm}^2\cdot\text{s}^{-1}$
293.2	0	3.12
303.2	0	2.35
323.2	0	1.39
343.3	0	0.90
303.2	0.12	2.42
323.2	0.12	1.45
343.2	0.12	0.95
293.2	5.00	5.32
303.2	5.00	4.18
323.2	5.00	2.33
343.2	5.00	1.37
303.2	11.07	6.00
323.2	11.07	3.39
343.2	11.07	1.91
278.3	11.12	14.2
293.2	11.12	8.44
303.2	11.12	5.93
323.2	11.12	3.33
343.2	11.12	1.96

Standard uncertainty
 $u(T) = 0.1 \text{ K}$. Expanded
 uncertainty
 $U(\nu) = 0.051 \text{ mm}^2\cdot\text{s}^{-1}$ (0.95
 level of confidence)

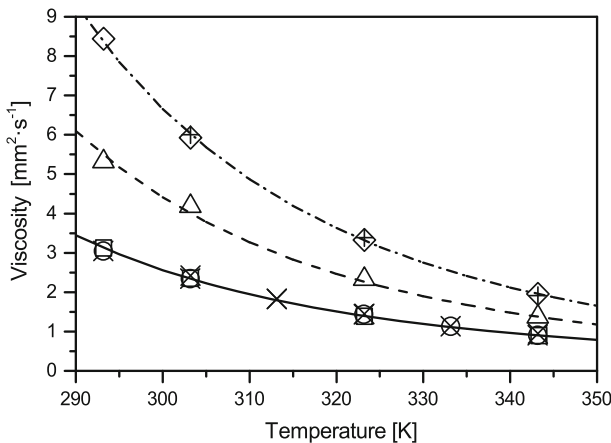


Fig. 10 Viscosity ν for the isopropanol/ Al_2O_3 nanofluid as a function of the mass fraction of nanoparticles $w_{\text{Al}_2\text{O}_3}$ and temperature : (\square) $w_{\text{Al}_2\text{O}_3} = 0 \text{ mass}\%$; (\circ) Stephan et al. [15]; $w_{\text{Al}_2\text{O}_3} = 0 \text{ mass}\%$; (\times) $w_{\text{Al}_2\text{O}_3} = 0.12 \text{ mass}\%$; (\triangle) $w_{\text{Al}_2\text{O}_3} = 5.00 \text{ mass}\%$; (\diamond) $w_{\text{Al}_2\text{O}_3} = 11.07 \text{ mass}\%$; ($+$) $w_{\text{Al}_2\text{O}_3} = 11.12 \text{ mass}\%$; (—) $w_{\text{Al}_2\text{O}_3} = 0 \text{ mass}\%$ by Eq. 7; (- - -) $w_{\text{Al}_2\text{O}_3} = 5.00 \text{ mass}\%$ by Eq. 7; (- · -) $w_{\text{Al}_2\text{O}_3} = 11.07 \text{ mass}\%$ by Eq. 7

The experimental data can be fitted using Eq. 7 with deviations $< 4.5\%$. The obtained viscosity values are in qualitative agreement with results of many studies summarized in reviews [27,28].

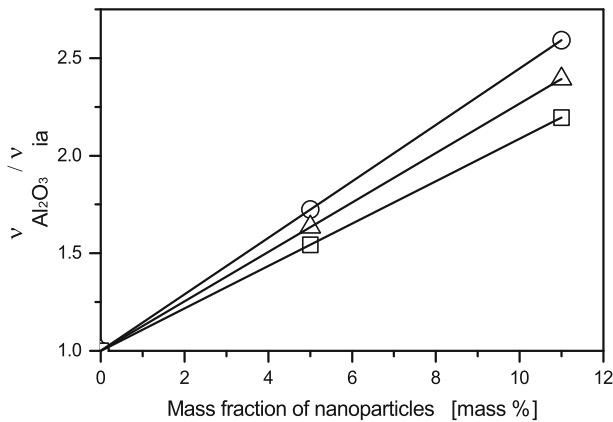


Fig. 11 Ratio $\nu_{Al_2O_3} / \nu_{ia}$ of nanofluid viscosity $\nu_{Al_2O_3}$ to the pure isopropanol viscosity ν_{ia} at the same temperatures depending on the mass fraction of nanoparticles: (○) = 300 K; (△) $T = 320$ K; (□) $T = 340$ K

3 Conclusions

The results of experimental study of the effect of nanoparticle additives on the density, saturated vapor pressure, surface tension and viscosity of isopropanol/ Al_2O_3 nanofluid were presented in this paper. Experiments have shown that the nanofluids remain stable over a wide range of concentrations and temperatures.

The main advantage of the experimental data presented is that the density, viscosity, surface tension and saturated vapor pressure data for isopropanol/ Al_2O_3 colloidal solutions were obtained for stable nanofluids and identical samples of a certain purity. The availability of experimental data obtained under consistent and reproducible conditions creates many opportunities for the development of new models for predicting properties of nanofluids.

In our opinion, future accurate prediction models should consider the temperature and concentration dependence of the hydrodynamic radius of nanoparticles and the structure of the nanofluid. The change of concentration of the surface layer of the nanofluid liquid phase, and the functional dependence of the saturated vapor pressure and surface tension should also be considered. These issues reflect our interests for further studies.

References

1. J.P. Hartnett, T.F. Irvine, G.A. Greene, Y.I. Cho, A. Bar-Cohen, *Advances in Heat Transfer* (Academic press, London, 2009)
2. J.P. Hartnett, T.F. Irvine, G.A. Greene, Y.I. Cho, *Advances in Heat Transfer* (Academic press, London, 2011)
3. W. Yu, D.M. France, J.L. Routbort, S.U. Choi, *Heat Transf. Eng.* **29**, 432 (2008)
4. X.Q. Wang, A.S. Mujumdar, *Int. J. Therm. Sci.* **46**, 1 (2007)
5. C.H. Li, G. Peterson, *J. Appl. Phys.* **101**, 044312 (2007)
6. E.V. Timofeeva, A.N. Gavrilov, J.M. McCloskey, Y.V. Tolmachev, S. Sprunt, L.M. Lopatina, J.V. Selinger, *Phys. Rev. E* **76**, 061203 (2007)

7. S.S. Murshed, S.H. Tan, N.T. Nguyen, J. Phys. D: Appl. Phys. **41**, 085502 (2008)
8. M. Bhuiyan, R. Saidur, R. Mostafizur, I. Mahbul, M. Amalina, Int. Commun. Heat Mass Transf. **65**, 82 (2015)
9. G.J. Tertsinidou, C.M. Tsolakidou, M. Pantzali, M.J. Assael, L. Colla, L. Fedele, S. Bobbo, W.A. Wakeham, J. Chem. Eng. Data **62**, 491 (2016)
10. K.D. Antoniadis, G.J. Tertsinidou, M.J. Assael, W.A. Wakeham, Int. J. Thermophys. **37**, 1 (2016)
11. C. Choi, H. Yoo, J. Oh, Curr. Appl. Phys. **8**, 710 (2008)
12. S. Tanvir, L. Qiao, Nanoscale Res. Lett. **7**, 226 (2012)
13. V. Zhelezny, N. Lukianov, O.Y. Khliyeva, A. Nikulina, A. Melnyk, Int. J. Refrig. **74**, 486 (2017)
14. R. Xu, R. Wang, W. Cong, G. Yan, Y. Wuny, in *Proceedings of International Congress of Refrigeration. ICR07-B1-1357* (2007)
15. P. Stephan, S. Kabelac, M. Kind, H. Martin, D. Mewes, K. Schaber, *VDI Heat Atlas* (Springer, Berlin, 2010)
16. A. Nikulin, O. Khliyeva, N. Lukianov, V. Zhelezny, Y. Semenyuk, Int. J. Heat Mass Transf. **118C**, 746 (2018)
17. T. Lozovsky, I. Motovoy, O. Khliyeva, V. Zhelezny, in *Proceedings of 3rd International Conference on Thermophysical and Mechanical Properties of Advanced Materials*. 59 (2016)
18. R. Vajjha, D. Das, B. Mahagaonkar, Pet. Sci. Technol. **27**, 612 (2009)
19. V. Zhelezny, Y.V. Semenyuk, S. Ancherbak, A. Grebenkov, O. Beliayeva, J. Fluor. Chem. **128**, 1029 (2007)
20. S. Vafaei, A. Purkayastha, A. Jain, G. Ramanath, T. Borca-Tasciuc, Nanotechnology **20**, 185702 (2009)
21. N. Ahammed, L.G. Asirvatham, S. Wongwises, J. Therm. Anal. Calorim. **123**, 1399 (2016)
22. M. Jarahnejad, E.B. Haghghi, M. Saleemi, N. Nikkam, R. Khodabandeh, B. Palm, M.S. Toprak, M. Muhammed, Rheol. Acta **54**, 411 (2015)
23. K. Anoop, T. Sundararajan, S.K. Das, Int. J. Heat Mass Transf. **52**, 2189 (2009)
24. W. Williams, J. Buongiorno, L.W. Hu, J. Heat Transf. **130**, 042412 (2008)
25. A.D. Sommers, K.L. Yerkes, J. Nanoparticle Res. **12**, 1003 (2010)
26. H. Chen, Y. Ding, C. Tan, New J. Phys. **9**, 367 (2007)
27. S. Murshed, K. Leong, C. Yang, Appl. Therm. Eng. **28**, 2109 (2008)
28. R. Saidur, K. Leong, H. Mohammad, Renew. Sustain. Energy Rev. **15**, 1646 (2011)